Journal of Alloys and Compounds 509 (2011) 4978–4986

Contents lists available at ScienceDirect

Journal of Alloys and Compounds

journal homepage: www.elsevier.com/locate/jallcom

Synthesis behavior of nanocrystalline Al–Al_2O_3 composite during low time mechanical milling process

Mostafa Alizadeh*, Morteza Mirzaei Aliabadi

Department of Materials Science and Engineering, International Center for Science, High Technology & Environmental Sciences, Kerman, Iran

ARTICLE INFO

Article history:
Received 24 June 2010
Received in revised form
24 December 2010
Accepted 30 January 2011
Available online 22 February 2011

Keywords:
Nanostructured materials
Metal matrix composites
Mechanical alloying

ABSTRACT

In this work, four different volume fractions of Al_2O_3 (10, 20, 30 and 40 vol.%) were mixed with the fine Al powder and the powder blends were milled for 5 h. Scanning electron microscopy analysis, particle size analysis and bulk density measurements were used to investigate the morphological changes and achieving the steady state conditions. The results showed that increasing the Al_2O_3 content can provide the steady state particle size in 5 h milling process. It was found that increasing the volume fraction of Al_2O_3 leads to increasing the uniformity of Al_2O_3. Standard deviations of microhardness measurements confirmed this result. The XRD pattern and XRF investigations depicted that increasing the Al_2O_3 content causes an increase in the crystal defects, micro-strain and Fe contamination during 5 h milling process of nanocrystalline composite powders while the grain size is decreased. To investigate the effect of milling time, Al–30 vol.% Al_2O_3 (which achieved steady state during 5 h milling process) was milled for 1–4 h. The results depicted that the milling time lower than 5 h, do not achieve to steady state conditions.

1. Introduction

Aluminum metal matrix composites are ideal materials for structural applications in aerospace, automotive and military industries due to their high mechanical properties such as strength, stiffness, wear resistance and good physical behaviors including light weight, and electrical and thermal conductivity [1–5]. Reinforcing the ductile aluminum matrix with stronger and stiffer second-phase reinforcements like Al_2O_3, SiC, AlN, Si_3N_4, Al_4C_3 and TiC provides a combination of properties of both metallic matrix and ceramic reinforcement components resulting in improved physical and mechanical properties of composite [6–11].

Al_2O_3 is known as a suitable reinforcement for the Al matrix since it is chemically inert with Al and can be also used in higher temperatures, in comparison with the un-reinforced aluminum, with accompanying benefits of resistance to creep [12]. Uniform dispersion of the Al_2O_3, particles with steady state conditions and a fine grain size of the matrix contribute to improve the mechanical properties of the composite. Further, mechanical properties of the composite tend to improve by increasing the volume fraction of the reinforcements [12–14]. Recently, nanostructured composites have been found considerable attention due to their unique mechanical behavior [15]. Mechanical alloying (MA) is a simple and useful technique for achieving a uniform distribution of the fine particles within nanocrystalline composites [12].

There exist numerous studies about Al–Al_2O_3 nanocrystalline composite investigating the steady state conditions [16–21]. For example, Razavi Tousi et al. used high energy ball milling to produce a nanostructured Al matrix composite reinforced by 20 wt% submicron Al_2O_3 particles. They showed that addition of alumina particles as the reinforcement has a strong effect on the size, morphology and pressability of the powder. They also worked to decrease the time taken to reach a steady state using the milling time and found for 20 wt% submicron Al_2O_3, after 10 h milling the steady state is achieved [22]. Suryanarayana studied the steady state conditions and concluded that with increasing the alumina amount the time taken to achieve steady state is decreased [12]. Razavi Hesabi evaluated the structural change during mechanical milling of nanometric and micrometric Al_2O_3 reinforced Al matrix composites and found when hard alumina particles are added to aluminum powder, the fracture occurs earlier, and thus the steady-state condition, i.e. formation of equiaxed particles, is achieved after shorter milling time. Zebarjad et al. investigated the microstructure of Al–Al_2O_3 composite produced by mechanical milling and found that increasing of milling time causes to make fine alumina powders and uniform its distribution. Also leads the composite towards steady state condition in which, all microstructure properties such as powder size, powder shape and distribution of alumina within aluminum remain fixed. They analyzed the initial and milled powders at different times and showed that at the beginning of milling the powders will tend to absorb iron and gradually their

* Corresponding author. Tel.: +98 3426226611; fax: +98 3426226617; mobile: +98 9133541004.
E-mail address: alizadeh@icst.ac.ir (M. Alizadeh).

0925-8388/$ – see front matter © 2011 Elsevier B.V. All rights reserved.
doi:10.1016/j.jallcom.2011.01.177

Table 1
The size distribution and purity of starting materials.

Material	D_{10} (μm)	D_{50} (μm)	D_{90} (μm)	Purity
Al	20.36	80.93	205.966	99.5%
Al_2O_3	4.674	15.743	44.105	99%

susceptibility decrease until steady state condition is prevailed [3].

Although there exist numerous investigations in the field of Al–Al_2O_3 nanocrystalline composite investigating the steady state conditions, however there is no sufficient information about low time milling in the literatures. The main goal of the present work is to investigate the synthesis behavior and steady state conditions of nanocrystalline Al–Al_2O_3 composites powders produced by low time milling process. It must be mentioned that one of the objectives during the present work is to find the volume fraction of Al_2O_3 in which the steady state of composite powders is achieved during a specified low time milling. Another aim in the present work is to ensure that after low time milling a homogeneous distribution of Al_2O_3 in the aluminum matrix is achieved. The reason behind this is the fact that a uniform distribution of reinforcements could potentially result in composites with improved mechanical properties.

2. Experimental procedure

Pure Al powder with the purity of 99.5% and fine Al_2O_3 powder with the purity of 99% were used as starting materials for milling operation. The particle size distribution of starting powders was determined using a laser particle size analyzer (Mastersizer 2000, Malvern Instruments, UK) and the results of this analysis are shown in Table 1.

The powder blends with composition of $Al_{(100-x)}$–$Al_2O_{3(x)}$ (x = 10, 20, 30 and 40 vol.%) were milled using a planetary ball mill (Fritsch GmbH, model 'Pulverisette 6') in a hardened chromium steel vial and balls (10 mm diameter). The milling process was carried out at 300 rpm under argon atmosphere. All samples were milled for 5 h with the ball to powder weight ratio 10:1. To investigate the effect of milling time (lower than 5 h) the 30 vol.% Al_2O_3 samples were milled for 1–4 h. To avoid any excessive cold welding of powder particles amongst themselves and internal surfaces of the vial, 2–4 wt% ethanol was used as the process control agent (PCA). As the volume fraction of Al_2O_3 was increased the amount of PCA also was increased.

The morphology of as received and milled powders was characterized using a scanning electron microscope (SEM, S360, Cambridge, UK). The distribution of Al_2O_3 particles in the Al matrix in the milled powder blends was obtained using the optical microscope (OM). The particle size distribution of milled powders was determined using the laser particle size analyzer (Mastersizer 2000, Malvern Instruments, UK).

The variation in bulk density of powders at the different volume fraction of Al_2O_3 was measured according to the standard Hall method (ASTM B417).

The hardness test was performed to measure the hardness of specimens using the Duramin-1 hardness tester at room temperature with a 100 gF load and a 15 s dwell time. Any hardness value was an average of ten measurements for each specimen.

X-ray diffraction (XRD) with a D8 Bruker diffractometer (40 kV and 40 mA) and Cu Kα radiation (λ = 0.154 nm) was used to analyze the crystal structure of the milled powders. The XRD patterns were recorded in the 2θ range of 30–120° with the step size of 0.01°. The grain size and lattice strain changes during the milling process were calculated by Williamson–Hall method for at least four peaks after removing instrumental broadening that was determined using the XRD pattern of an annealed Al powder. The X-ray fluorescence investigation was done using XRF (XMF 104-Unisantis-Germany) to chemical analysis of the milled samples.

3. Results and discussion

3.1. Evolution of morphology

Fig. 1 shows the SEM image of as received Al (Fig. 1a) and Al_2O_3 (Fig. 1b) powders. This figure confirms the results of Table 1. As it can be seen, the as received Al powder includes a wide size distribution of plate-like particles and the as received Al_2O_3 powders exhibit a narrow distribution of irregular shaped particles. Since the Al particle size is almost five times more than Al_2O_3 particle size (see also Table 1), the SEM micrograph of Al powders is taken with a less magnification.

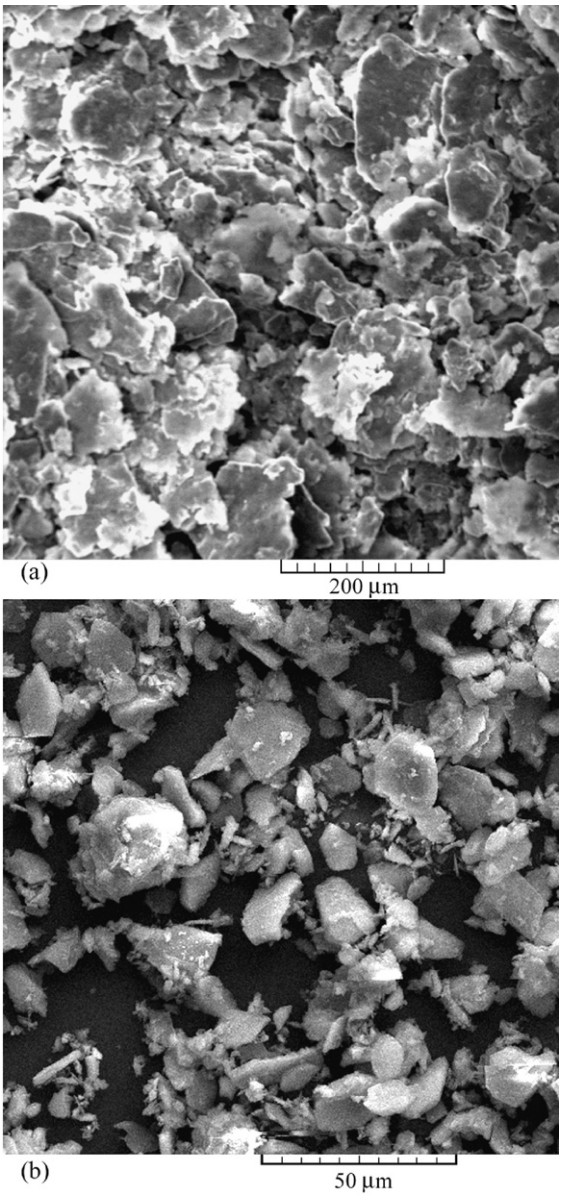

Fig. 1. SEM micrograph of starting powders: (a) Al and (b) Al_2O_3.

Fig. 2a and d shows the SEM micrographs of Al–Al_2O_3 composite particles containing 10, 20, 30 and 40 vol.% Al_2O_3 milled for 5 h. These figures depict the effect of Al_2O_3 content on the morphological changes during 5 h milling. Comparing Fig. 1a and Fig. 2a and d reveal that 5 h milling the Al particles together with the Al_2O_3 particles causes elimination of plate-like morphology of particles. According to Fig. 2a and d, increasing the volume fraction of Al_2O_3 causes an increased agglomeration in the composite powders produced during 5 h milling. Moreover, it can be found from Fig. 2a and d that the composite particle size is a function of Al_2O_3 content.

In order to quantify the effect of Al_2O_3 amount on the composite particle size, the median size (D_{50}) of 5 h milled powders including 0, 10, 20, 30 and 40 vol.% Al_2O_3 were determined using the laser particle size analyzer. The results of this analysis are shown by Fig. 3. As it can be seen from Fig. 3, increasing the Al_2O_3 amount from 0 up to 20 vol.% causes a considerable decrease in the composite particle size while after that the composite particle size do not change with Al_2O_3 amount.

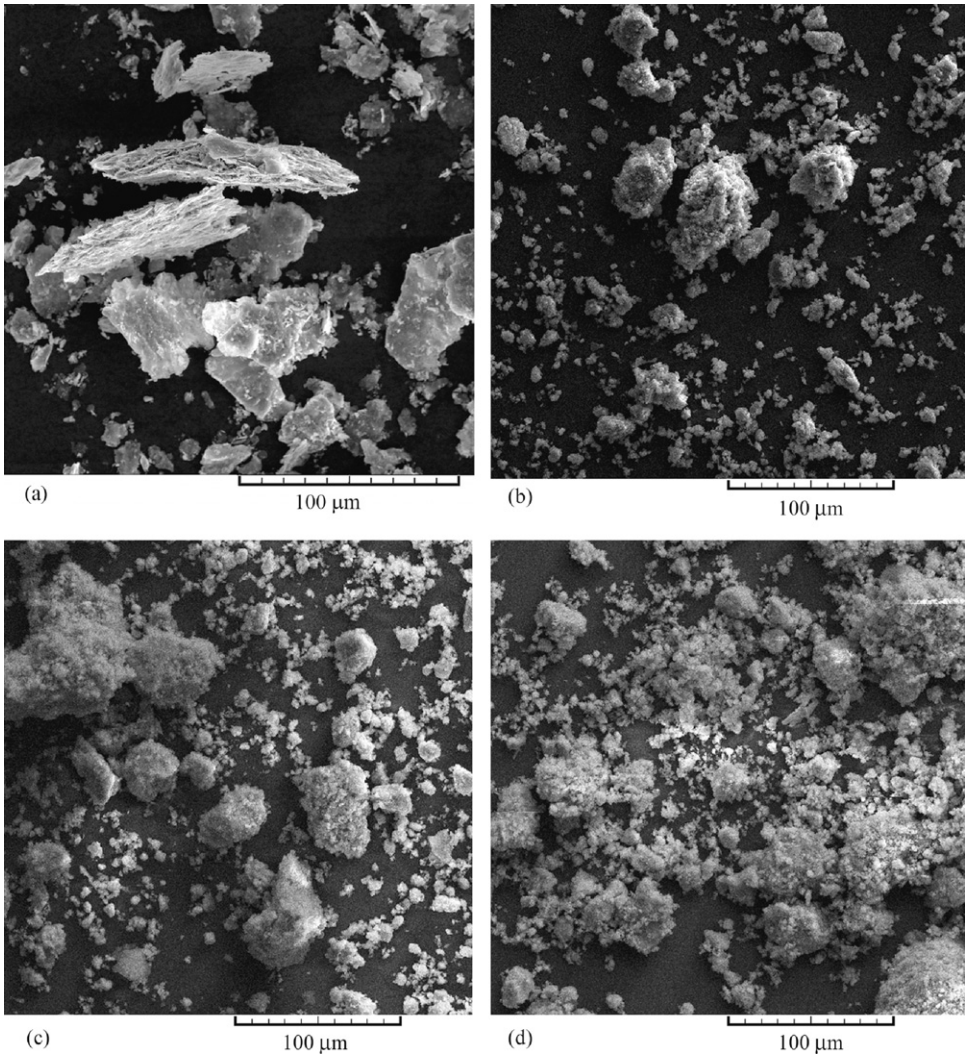

Fig. 2. SEM images of composite powder after 5 h ball milling for: (a) 10 vol.% Al_2O_3, (b) 20 vol.% Al_2O_3, (c) 30 vol.% Al_2O_3 and (d) 40 vol.% Al_2O_3.

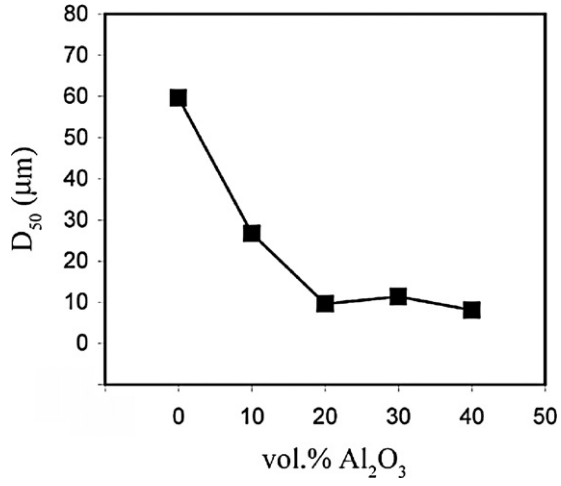

Fig. 3. Median size of 5 h milled pure Al and Al–Al_2O_3 composite powders.

The results mentioned above may be justified as follows: during MA of this system, the Al powders with Al_2O_3 particles sticking onto them are cold welded with other surfaces. As a result, the Al_2O_3 particles are entrapped in the Al matrix and provide easier propagation of cracks in the Al matrix under cyclic loading during the milling process. This phenomenon is intensified by cold working induced during MA process [23]. Therefore, in the Al–Al_2O_3 system, particle deformation-cold welding and fracture are two mechanisms which take place through milling process. When the Al_2O_3 content is low, the Al particle deformation and cold welding are predominant mechanisms [13]. Due to this causes, the composite powders with 10 vol.% Al_2O_3 include relatively large irregular (less equiaxed) particles (see Fig. 2a) compared to those with higher Al_2O_3 contents (see Fig. 2d). By increasing the Al_2O_3 content, contribution of the fracture mechanism is increased and consequently the particle size is more decreased. Moreover, the presence of Al_2O_3 particles increases the local deformation of the Al matrix enhancing the work hardening rate of the Al matrix, changing the slip characteristics and increasing the yield point [24]. Therefore, it is reasonable to believe that the presence of Al_2O_3 particles leads to decreasing the fracture toughness of the Al powders increasing their fracture during milling. Moreover, there exists the phenomenon of size reduction by breaking the hard (Al_2O_3) particles. This phenomenon is intensified when the volume fraction of Al_2O_3 is increased. Consequently increasing the volume fraction of Al_2O_3 particles leads to a decrease in the particle size of the composite powder during the low time milling. According to Fig. 3, this decreasing is continued until creation of a balance between the rate of welding and fracturing. This behavior may be related to the steady state achieving in the composite particle size.

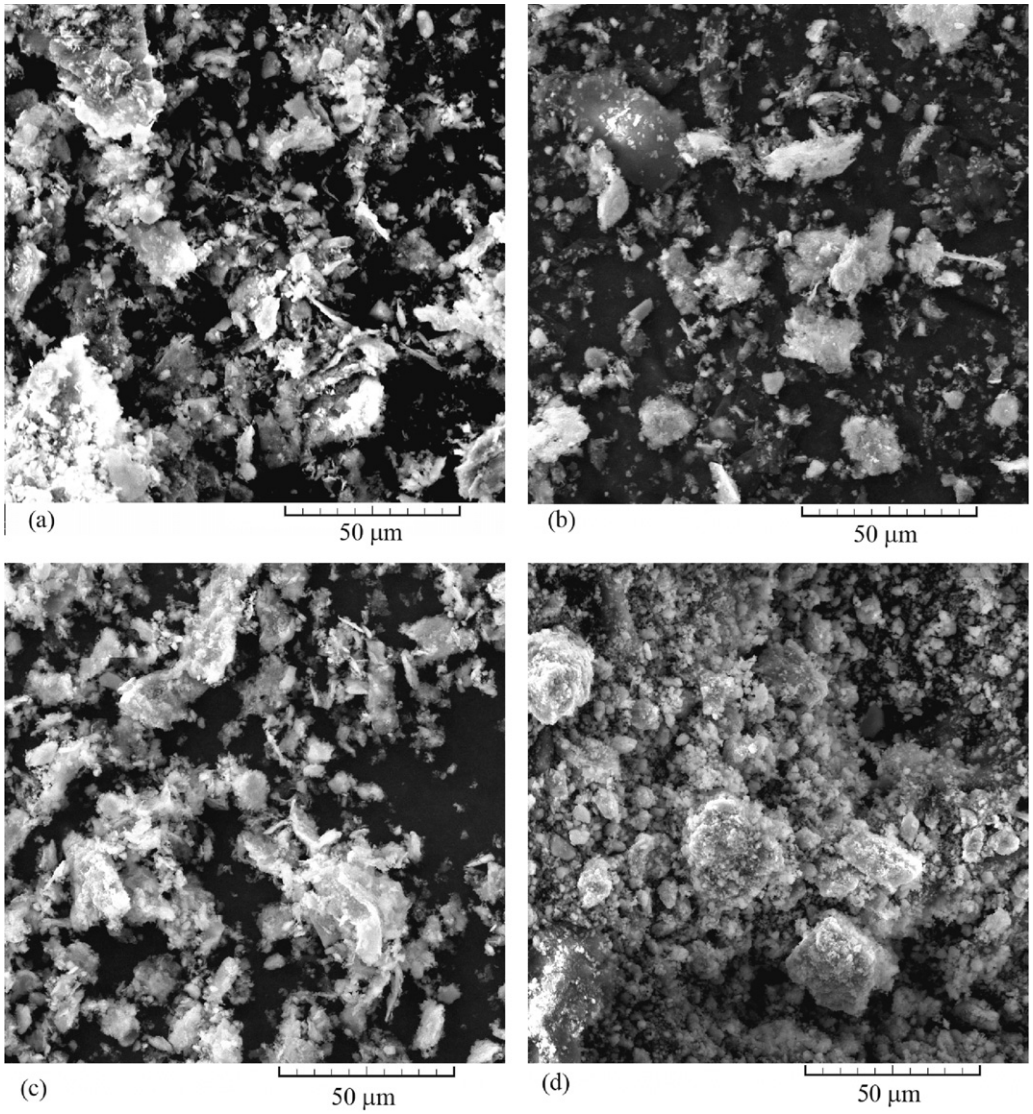

Fig. 4. SEM images of powders including 30 vol.% Al_2O_3 milled for 1–4 h.

As mentioned already, the purpose of this work is to study the nanocrystalline composite powder during low time milling process. So it is necessary to investigate the milling time lower than 5 h. To evaluate the effect of milling time, four samples including 30 vol.% Al_2O_3 were milled for 1–4 h. Fig. 4a and d shows the SEM micrographs of these samples. It can be found from these figures that the composite particle size is a function of milling time. With increasing the milling time, the composite particle size is decreased. Also, some agglomerated powders are seen in the 4 h milled composite powders.

To quantify the effect of low time milling on the composite particle size, the median size (D_{50}) of 30 vol.% Al_2O_3 powders milled for 1–4 h were determined using the laser particle size analyzer. The results of this analysis are shown by Fig. 5. Generally, the results show that increasing the milling time from 1 up to 4 h causes a decrease in the composite particle size. The milling times of 1, 2 and 3 h are not adequate to create a considerable decreasing in the D_{50}. While after 3 h milling, there exist a considerable decreasing in the median size of 30 vol.% Al_2O_3 powders. This figure also shows the amount of D_{50} for 5 h milled powders with same volume percentage of Al_2O_3. As it can be seen the decreasing of D_{50} is continued also until the 5 h milling time. However this figure reveals that the D_{50} for 4 and 5 h milled samples are near together.

To study the steady state achieving, one can evaluate the variation in the bulk density of powders during the MA process [25]. It is known that the powder density depends on the size, morphology, and size distribution of its particles. Therefore, a change in the

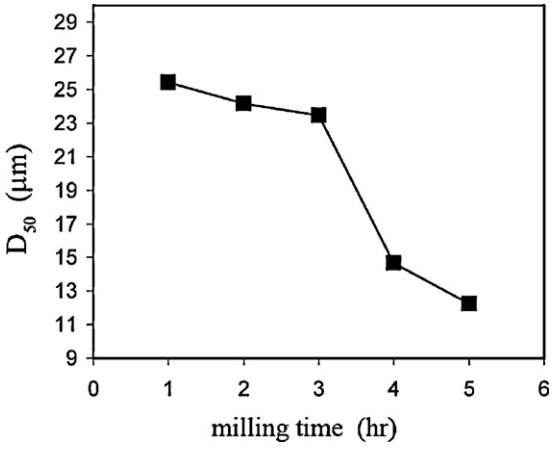

Fig. 5. The median size of 30 vol.% Al_2O_3 powders milled for 1–4 h.

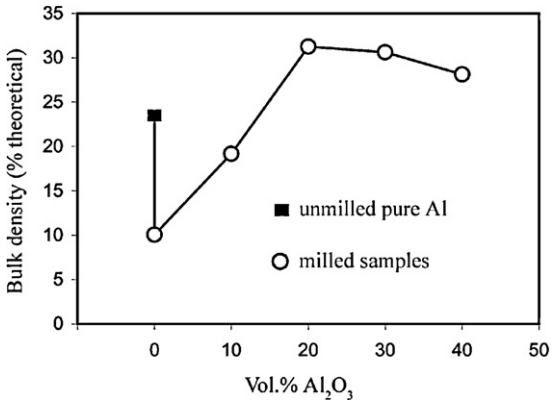

Fig. 6. The bulk density of Al–Al_2O_3 composite powder as function of volume fraction of Al_2O_3.

bulk density of powders during MA means that the particles morphology is changing. In other words, the steady state has not been achieved yet. Vice versa, the steady state of particle size has been achieved [25,26]. Fig. 6 shows the bulk density of unmilled pure Al powders (black square sign) and the 5 h milled powders including 0, 10, 20, 30 and 40 vol.% Al_2O_3 (white circle sign). This figure shows that 5 h milling of pure Al causes a considerable decrease in the density of the powders. As it can be seen, the density from 25% of the theoretical value (for unmilled pure Al) drops to 10% of the theoretical value (for milled pure Al). This reduction is related to the morphology of pure Al after 5 h milling process. Fig. 7 shows the SEM image of pure Al milled for 5 h. Comparing Figs. 1a and 7 show that after 5 h milling of pure Al, the particles are deformed and a more flattening is noticed. This phenomenon results in the reduction of density of the milled powder. According to Fig. 6, when the volume fraction of Al_2O_3 is increased from 0 up to 20 vol.%, a considerable increase is observed in the bulk density of 5 h milled powders. After that, the density shows a slight decrease which can be related to the agglomeration of milled powders containing 30 and 40 vol.% Al_2O_3 (see Fig. 2c and d). In fact, it can be resulted from Fig. 6 that the steady state is achieved in the 20 vol.% Al_2O_3. This result confirms the result of Fig. 3.

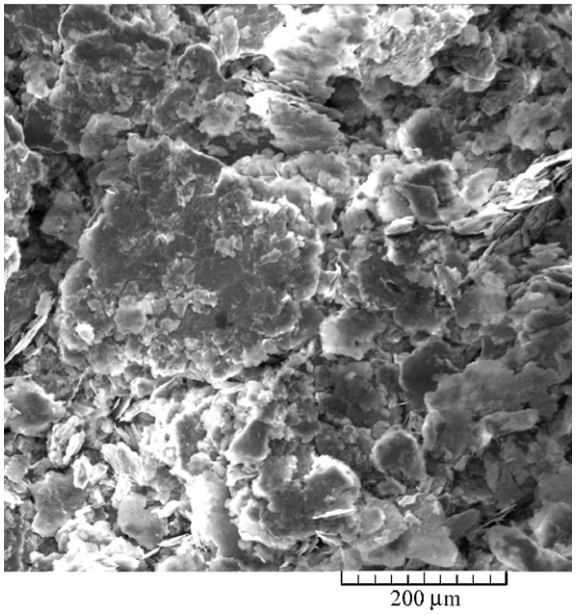

Fig. 7. SEM micrograph of pure Al (0 vol.% Al_2O_3) after 5 h milling.

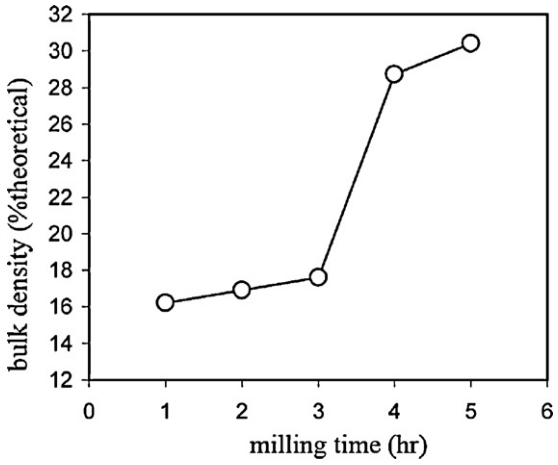

Fig. 8. Variation of bulk density versus the milling time for the samples including 30 vol.% Al_2O_3.

Fig. 8 shows the variation of bulk density versus the milling time for the samples including 30 vol.% Al_2O_3. According to this figure, generally the bulk density is increased with milling time. However, from 1 up to 3 h milling times, the bulk density increased slowly, while after 3 h a considerable increasing is seen in the bulk density of composite powders. In this figure, the variation of bulk density is continued until 5 h milling time. Although increasing of bulk density is continued also up to 5 h milling time, however its values for 4 and 5 h milled samples are near together. This means the 4 h milled powders is closed to the steady state conditions.

3.2. Embedding of Al_2O_3 particles within Al powders

One of the objectives in the present work is to ensure that after low time milling process a homogeneous distribution of Al_2O_3 in the aluminum matrix is achieved. To confirm that this distribution is uniform OM images of samples were provided. Fig. 9 shows the OM images of the nanocrystalline Al–Al_2O_3 composite with different volume fractions of Al_2O_3 milled for 5 h. The sample with 10 vol.% Al_2O_3 includes the Al_2O_3 particles with a relatively broad size distribution. As it can be seen from Fig. 9a, the particles A, B and C is almost ~44, ~21 and ~9 μm in diameter respectively. As it can be seen, the 5 h milled samples with 20, 30 and 40 vol.% Al_2O_3 include approximately uniform size and distribution of Al_2O_3. In fact, during milling of these samples the Al_2O_3 particles are broken and their size is decreased. However in the samples with 40 vol.% Al_2O_3 there exist some agglomerated region that can be related to the fining of Al_2O_3 particles during milling process.

As mentioned before, the uniformity of the reinforcement influences the mechanical properties of the composite. Fig. 10 illustrates the hardness behavior of the composites as a function of volume fraction of Al_2O_3. Each microhardness point in this diagram is an average of 10 measurements. This figure also depicts the standard deviations (SD) of microhardness measurements. As Fig. 10 shows, when the volume fraction of Al_2O_3 is increased from 10 up to 40 vol.%, the hardness of composite is increased from 121.2 up to 164.9 HV. The noticeable point in this figure is the behavior of standard deviations versus volume fraction of Al_2O_3. As it can be seen, when the volume fraction of Al_2O_3 is increased up to 20 vol.%, a severe decrease is observed in the SD while after that the SD of microhardness shows a slight change. Decreasing the SD means that uniformity of Al_2O_3 distribution in the Al matrix is increased. Thus it can be confirmed that increasing the Al_2O_3 content leads to increasing its uniformity.

Fig. 11 depicts the OM images of samples including 30 vol.% Al_2O_3 milled for 1–4 h. As it can be seen, the sample milled for 1 h

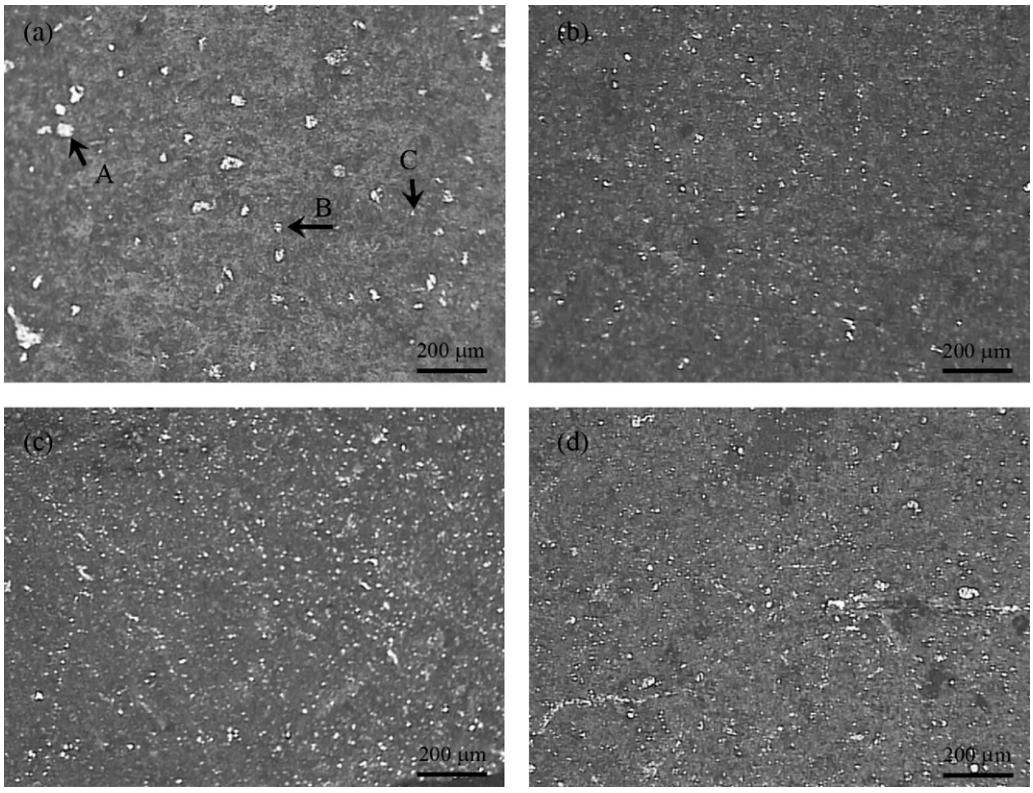

Fig. 9. The OM images of the composite with different volume fractions of Al_2O_3 milled for 5 h.

includes non-uniformly dispersed Al_2O_3 particles. With increasing the volume percentage of Al_2O_3 its uniformity is increased. Fig. 11d shows that the sample milled for 4 h includes approximately uniform size and distribution of Al_2O_3 particles. The variation of hardness and its SD for the 30 vol.% Al_2O_3 samples milled for 1–4 h are illustrated in Fig. 12. In general, increasing the milling time from 1 up to 4 h causes an increase in the hardness. Variation of hardness and its SD is continued up to 5 h (with the same volume percentage of Al_2O_3). As it can be seen the increasing of hardness is continued also for 5 h milling time. However this figure reveals that the hardness for 4 and 5 h milled samples are near together. The standard deviation shows a continuous decreasing with increasing the milling time. As a result of this figure, it can be seen that there is no uniformity in the hardness and SD for the samples milled for the times lower than 5 h.

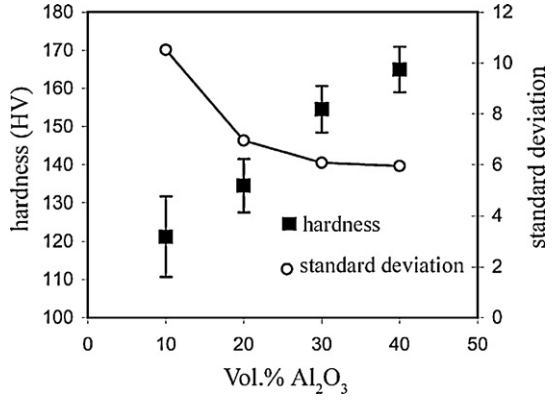

Fig. 10. Variation of hardness and standard deviation (SD) with volume fraction of Al_2O_3.

3.3. Grain refinement and structural evaluation

The above investigations show that the milling time less than 5 h is not suitable to produce uniform composite powder. Therefore to investigate the grain refinement, the 5 h milled samples are studied and the effect of volume percentage of Al_2O_3 is investigated.

Fig. 13 shows the XRD plots taken from Al–Al_2O_3 powder including different Al_2O_3 contents milled for 5 h. The structural evaluation and grain refinement are investigated using this figure. Investigation of Fig. 13 reveals that during 5 h milling, with increasing the volume fraction of Al_2O_3, a slight shift in the position of the Al peaks is noticed and the Al peaks are also broadened. For example, Fig. 14 shows the variation of Al peak broadening and displacement for the plane of (1 1 1). This figure includes the XRD peak of unmilled pure Al (peak a) and the XRD peaks of the samples including 0, 10, 20, 30 and 40 vol.% Al_2O_3 milled for 5 h (peaks b–f). As it can be seen, the peak broadening is increased with increasing the volume fraction of Al_2O_3. Moreover, with increasing the Al_2O_3 content, the peaks show a shift towards the higher angles. Table 2 shows the results of XRF investigations. As the XRF measurements reveals, increasing the Al_2O_3 content leads to increasing the Fe content in the composite powders. So the Al peak displacement can be related to dissolution of Fe contamination into the milled powder. Fig. 15 shows the Al peak displacement for the three main Al peaks (the planes of (1 1 1), (2 0 0) and (2 2 0)). Figs. 15 and 14 show that the peak position of 5 h milled pure Al (0 vol.% Al_2O_3) powders is near to that for the unmilled pure Al powders. On the contrary, when 10 vol.% Al_2O_3 is added, a considerable displacement is observed.

Table 2
The results of XRF investigations for the samples including various Al_2O_3 contents.

vol.% Al_2O_3	10	20	30	40
wt% Fe	1.35	1.71	1.88	1.91

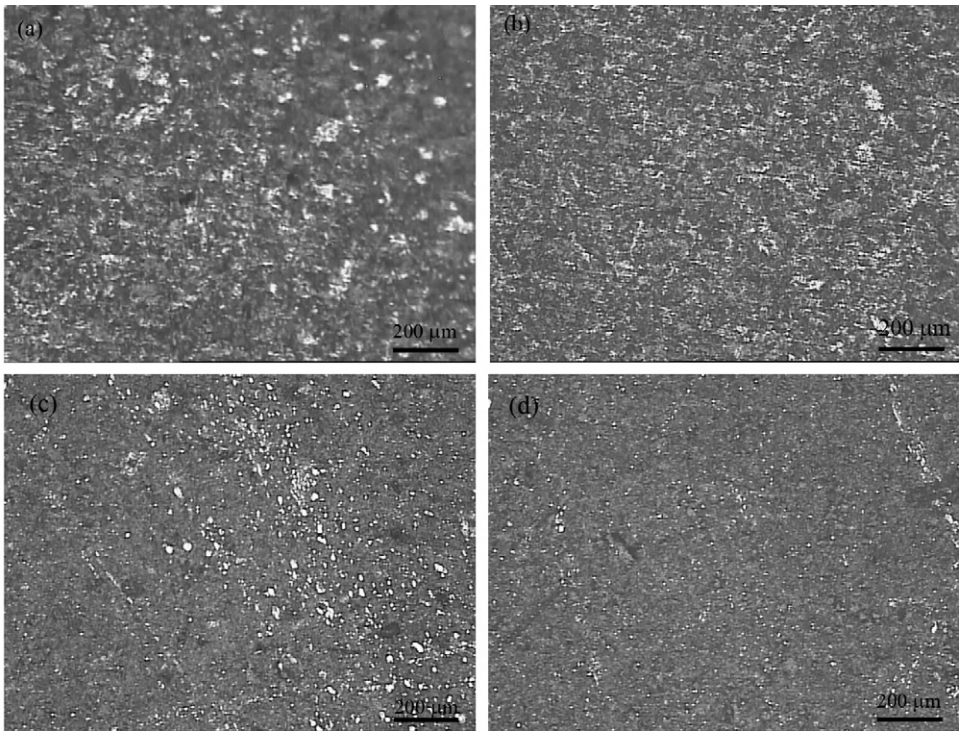

Fig. 11. The OM images of samples including 30 vol.% Al_2O_3 milled for 1–4 h.

This means that the presence of Al_2O_3 has a considerable effect on the formation of crystal defects during 5 h milling. Also, Fig. 15 illustrates that when the Al_2O_3 content is increased, the rate of peak displacement is decreased. This means that with increasing the Al_2O_3 content, the rate of crystal defect formation is decreased.

The grain size of Al powders was calculated using the XRD pattern (Fig. 13) by William–Hall method [27] via following equation:

$$\beta_s \cos\theta = \frac{k\lambda}{d} + 2\varepsilon \sin\theta \quad (1)$$

where β_s is the peak broadening in radians, θ is the position of peak maximum, K is the Scherrer constant (0.9), λ is the X-ray wavelength (λ Cu $K_{\alpha 1}$ = 0.15406 nm), d is the crystallite dimension and ε is an approximate upper limit of the lattice distortion. The instrumental broadening (β_i) was removed by applying the following equation according to Gaussian–Gaussian relationship using an annealed aluminum powder:

$$\beta_s^2 = \beta_e^2 - \beta_i^2 \quad (2)$$

where β_e is the FWHM (full width at half maximum) of the measured XRD peak.

Fig. 16 shows the crystallite size and lattice strain as functions of volume fraction of Al_2O_3. The results show that due to increasing the alumina from 10 vol.% up to 40 vol.%, the grain size of monolithic aluminum particles decreases from 114 nm to 93 nm at a constant milling time. Also the lattice strain increases from 0.87% to 1.1%. The interaction of the dislocations (generated during MA process) with the hard particles generates sub-boundaries which in turn results in the decomposition of the initial large grains into smaller ones. The decreased size of the Al grain when milled at the presence of

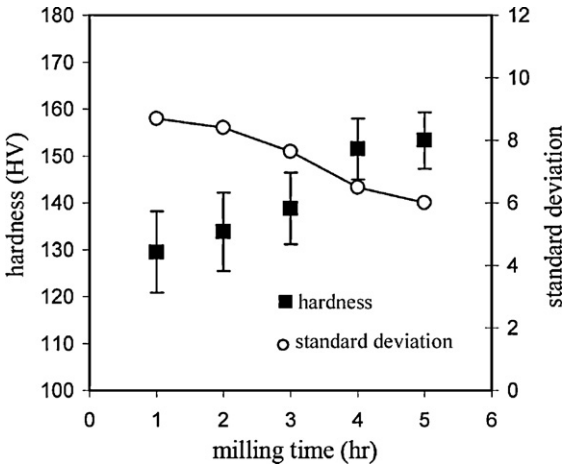

Fig. 12. Variation of hardness and its SD for the 30 vol.% Al_2O_3 samples milled for 1–4 h.

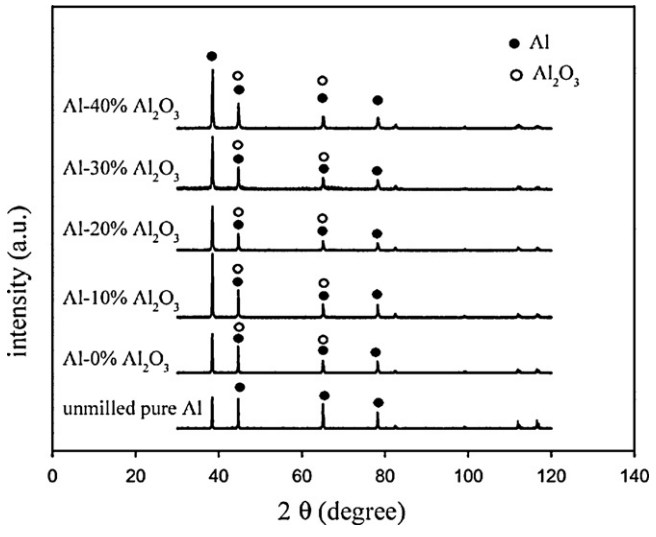

Fig. 13. XRD patterns of Al–Al_2O_3 powder for different Al_2O_3 contents after 5 h milling times.

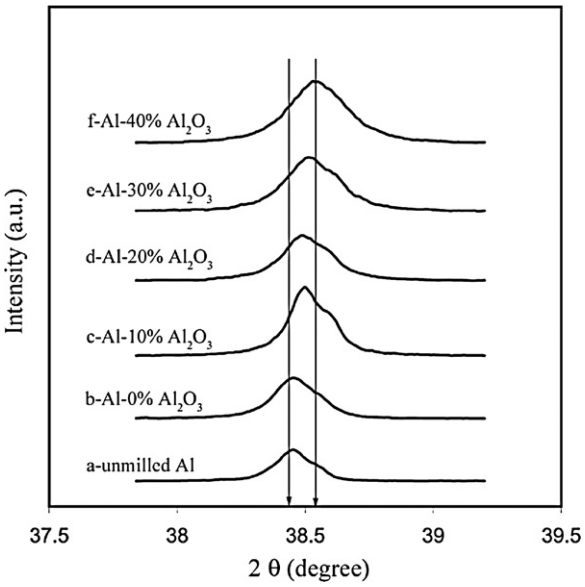

Fig. 14. XRD main peak of Al representing the peak broadening and displacement versus increasing the Al_2O_3 content.

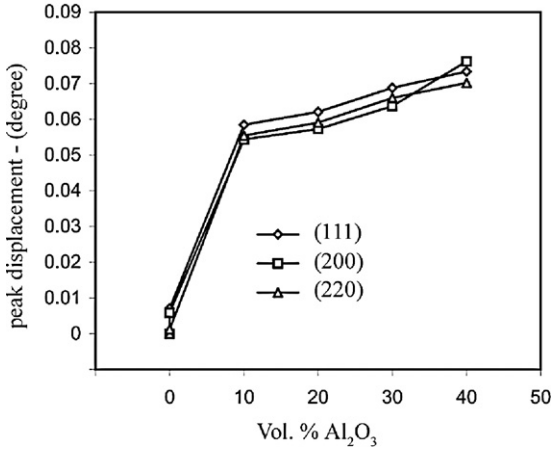

Fig. 15. Displacement of (1 1 1), (2 0 0) and (2 2 0) Al peaks as a function of volume fraction of Al_2O_3.

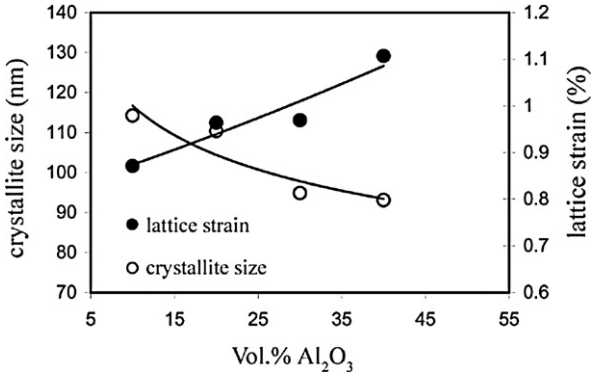

Fig. 16. Crystallite size and lattice strain as functions of volume fraction of Al_2O_3.

the hard Al_2O_3 particles can be in part attributed to hindering the dislocation movement by Orowan bowing mechanism, leading to an increase in the dislocation density thereby accelerating the grain refining progress.

4. Conclusions

The low time milling process was employed to investigate the synthesis behavior of nanocrystalline Al–Al_2O_3 composite powder. The following results can be listed briefly:

1. For 5 h milling, as the volume fraction of Al_2O_3 is increased the particle size of nanocrystalline composite is decreased and the agglomeration of the particles is increased.
2. The particle size decreasing is continued until creation of a balance between the rate of welding and fracturing. This behavior can be related to the steady state reaching in the composite particle size.
3. As the volume fraction of Al_2O_3 is increased, the morphology of composite powders is changed from plate like to a shape near the equiaxed.
4. The results of median size measurements and bulk density showed that for 5 h milling process the steady state is achieved at 20 vol.% Al_2O_3
5. For 5 h milling process, increasing the volume fraction of Al_2O_3 improves the distribution of Al_2O_3 in the Al matrix. However, there is not a considerable nonuniformity of Al_2O_3 in the low volume fraction. Thus it can be concluded that 5 h milling process can be suitable to produce a uniform nanocrystalline Al–Al_2O_3 composite.
6. For the composite powders including 30 vol.% Al_2O_3 (which achieved steady state during 5 h milling process) the milling times less than 5 h, do not reach to steady state conditions.
7. At a low time milling process, increasing the volume fraction of Al_2O_3 leads to an increase in the crystal defects.
8. During 5 h milling process, due to increasing the Al_2O_3 amount from 10 vol.% up to 40 vol.%, the grain size of monolithic Al particles decreased from 114 nm to 93 nm and also the lattice strain increased from 0.87% to 1.1%.
9. This study showed that during low time milling process, the steady state conditions may be attained in the high volume percentage of Al_2O_3.
10. Especially in this research, the 5 h milling of 20 and 30 vol.% Al_2O_3 composite is suggested and other milling times (1–4) and volume percentages of Al_2O_3 are not recommended for manufacturing of low time milled nanocrystalline composite powders.

Acknowledgement

The authors would like to acknowledge the authorities of the International Center for Science, High Technology & Environmental Sciences because of their efforts in providing the financial support of this work.

References

[1] L. Lu, M.O. Lai, C.W. Ng, Mater. Sci. Eng. A252 (1998) 203–211.
[2] K.H. Min, S.P. Kang, D.G. Kim, Y.D. Kim, J. Alloys Compd. 400 (2005) 150–153.
[3] S.M. Zebarjad, S.A. Sajjadi, Mater. Des. 27 (2006) 684–688.
[4] C. Nie, J. Gua, J. Liu, Di Zhang, J. Alloys Compd. 454 (2008) 118–122.
[5] M. Rahimian, N. Ehsani, N. Parvin, H.R. Baharvandi, Mater. Des. 30 (2009) 3333–3337.
[6] R. Narayanasamy, T. Ramesh, K.S. Pandey, Mater. Des. 27 (2006) 566–575.
[7] N. Zhao, Philip Nash, Xianjin Yang, J. Mater. Process. Technol. 170 (2005) 586–592.
[8] H. Abdoli, E. Salahi, H. Farnoush, K. Pourazrang, J. Alloys Compd. 461 (2008) 166–172.
[9] H. Arik, Y. Ozcatalbas, M. Turker, Mater. Des. 27 (2006) 799–804.
[10] Y. Ozcatalbas, Compos. Sci. Technol. 63 (2003) 53–61.
[11] Q. Hua, P. Luo, Y. Yan, Mater. Sci. Eng. A 486 (2008) 215–221.
[12] B. Prabhu, C. Suryanarayana, L. Ana, R. Vaidyanathan, Mater. Sci. Eng. A 425 (2006) 192–200.
[13] Z. Razavi Hesabi, A. Simchi, S.M. Seyed Reihani, Mater. Sci. Eng. A 428 (2006) 159–168.

[14] Z. Razavi Hesabi, H.R. Hafizpour, A. Simchi, Mater. Sci. Eng. A 454–455 (2007) 89–98.
[15] M.O. Lai, L. Lu, W. Laing, Compos. Struct. 66 (2004) 301–304.
[16] J.S. Benjamin, M.J. Bamford, Metall. Trans. A 8 (1997) 1301–1305.
[17] M.H. Enayati, Z. Rahmani, Mater. Sci. Eng. A 25 (2004) 515–521.
[18] S. Kleiner, F. Bertocco, F.A. Khalid, O. Beffort, Mater. Chem. Phys. 89 (2005) 362–366.
[19] E.M. Ruiz-Navas, J.B. Fogagnolo, F. Velasco, L. Froyn, Composites Part A 37 (2006) 2114–2120.
[20] C. Suryanarayana, Prog. Mater. Sci. 46 (2001) 1–184.
[21] S.M. Zebarjad, S.A. Sajjadi, Mater. Des. 28 (2007) 2113–2120.
[22] S.S. Razavi Tousi, R. Yazdani Rad, E. Salahi, I. Mobasherpour, M. Razavi, Powder Technol. 192 (2009) 346–351.
[23] M. Khakbiz, F. Akhlaghi, J. Alloys Compd. 479 (2009) 334–341.
[24] D.L. Davidson, in: R.K. Everett, R.J. Arsenault (Eds.), Metal Matrix Composites, Mechanisms and Properties, Academic Press, 1991, p. 217.
[25] J.B. Fogagnolo, F. Velasco, M.H. Robert, J.M. Torralba, Mater. Sci. Eng. A342 (2003) 131–143.
[26] J.B. Fogagnolo, E.M. Ruiz-Navas, M.H. Robert, J.M. Torralba, Mater. Sci. Eng. A355 (2003) 50–55.
[27] G.K. Williamson, W.H. Hall, Acta Metall. 1 (1953) 22–31.